Analog Maximum Power Point Tracking for Spacecraft within a Low Earth Orbit (February 2016)

David Selčan, Gregor Kirbiš and Iztok Kramberger, *Member*, IEEE, University of Maribor

***Abstract*—This paper describes the implementation of a reliable Maximum Power Point Tracking design implemented as an analog circuit for use on a satellite relying on solar power generation within Low Earth Orbit. The environment is evaluated within which such a spacecraft system would function. A specific Maximum Power Point Tracking algorithm is selected with regards to environmental constraints. A further increase in reliability was achieved by only using carefully selected analog components which are suitable for use within a space environment. The system was prototyped and its power conversion performance characterized using a custom built measurement setup. The system successfully tracked the Maximum Power Point through all the performed measurements. The results from the measurements suggest that the prototyped system has a nominal regulator efficiency of 88 % and a nominal tracking accuracy of 96 %.**

***Index Terms*—Satellites, Analog circuits, Power conversion, Maximum power point trackers, Solar power generation.**

I. Introduction

MOST satellites in orbit today rely on solar panels to generate the power necessary for their normal operation. This trend is unlikely to change since there is a distinct lack of alternative power sources in space. As such, the development of solar power generation technology for satellites remains of crucial importance for producing cheaper, more reliable spacecraft.

The current solar power generation topologies on board satellites can be split into two categories: the first consists of satellites which perform a direct transfer of power to the battery without applying any power shaping. While this direct load topology is extremely reliable, it suffers from a lack of efficiency. This is especially evident during Low Earth Orbit (LEO) missions, where a satellite can spend up to 50% of its time eclipsed by the Earth.

Therefore, the temperatures and illuminations of the solar panels fluctuate during each orbit cycle, meaning that the maximum amount of power that can be drawn from the solar panels also varies considerably. Since the direct load topology performs no power shaping, a lot of the maximum power that could otherwise be drawn is instead dissipated as heat on the solar panels themselves.

In order to counteract this effect, a different type of solar power generation topology has begun to be used in various forms. It relies on Maximum Power Point Tracking (MPPT) systems to shape the power generated by the solar panels. While this allows the satellite to draw most of the available power from the solar panels, this increase in efficiency does come a t a price. Current implementations of MPPT systems for satellites mostly make use of embedded systems with the MPPT algorithms implemented using a microcontroller. This brings forth two issues: in order to achieve the same response time to a change in solar panel conditions, digital implementations of MPPT algorithms have a higher implementation complexity than analog ones [1]. As such, the use of a digital implementation of a spacecraft MPPT system results either in a MPPT system that is very complex in its implementation (an example can be seen in [2] or in [3]), or isn't well adapted to operation in a rapidly changing environmental conditions, e.g. when the satellite is tumbling. The second issue is the existence of Single Event Effects (SEE), which are radiation induced occurrences that can be hazardous to microcontrollers if they have not been hardened against them.

The disadvantages of such MPPT implementations can be mitigated by using radiation-hardened microcontrollers in combination with sophisticated MPPT algorithms. This however increases the cost and also the complexity of the whole system, making it less suitable for highly reliable satellite systems. Such an increase in complexity is especially undesirable, since it can be very difficult to achieve reliable operation of a complex system.

In the light of this, we propose a solution in the form of an analog MPPT system. Such a system is able to react almost instantly to any changes in solar panels' temperatures and illuminations, instead of having to wait for the next sampling interval. The use of carefully selected analog components also makes the system immune to latch-up and most other radiation induced effects.

Manuscript received April 7, 2014; revised October 2, 2014, January 7, 2015, April 20, 2015; released for publication August 29, 2015.

DOI. No. 10.1109/TAES.2015.140279.

Refereeing of this contribution was handled by M. Veerachary.

Authors' address: University of Maribor, Faculty of Electrical Engineering and Computer Science Laboratory of Electronic and Information Systems, Smetanova 17, Maribor, 2000 Slovenia, E-mail: (david.selcan@um.si).

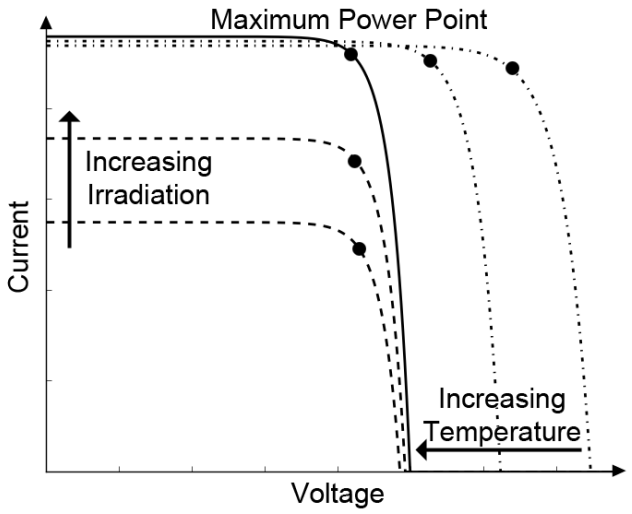

Fig. 1. I-V curve of a solar panel. The figure illustrates how temperature and illumination affect the characteristic of a solar panel, as well as its' MPP.

II. MPPT ALGORITHM DESIGN

The reason why direct load topology is not particularly well-suited for fully utilizing all the available power from a solar panel lies in the fact that the current-voltage (I-V) characteristic varies greatly with the temperature of the panel, as well as the amount of light illuminating it. A simplified explanation of these effects is that the open circuit (OC) voltage increases with decreasing temperature, while the short circuit (SC) current increases with increasing solar illumination (see Fig. 1). As such, there is one maximum power point (MPP) for each pair of illumination and temperature conditions. The I-V characteristic retains the shape of an exponential function independent of the parameters. This means that the MPP is always located at the knee of the I-V curve.

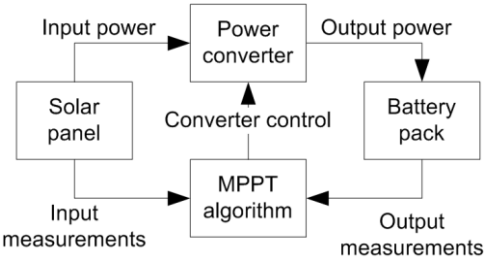

Fig. 2. Block diagram of a general MPPT algorithm implementation for use on a satellite.

MPPT algorithm implementation consists of a power converter, which is used to control the operating point of the solar panel, and a regulation system which is used to control the power converter, as can be seen in Fig. 2.

Since the I-V characteristic of a solar panel is also influenced by other parameters, like process variations, aging, cell degradation etc. MPPT algorithms are not well suited for implementation as an open loop control system (though there exist complex methods which use neural networks and fuzzy control, e. g. [4]). Due to this fact, most MPPT algorithms use a closed loop approach, measuring the input power of the solar panel and using it as the control variable.

A. Design considerations for space electronics

Space is a harsh environment for any electronic system. This especially holds true for a system that is vital for proper operation of the whole spacecraft. A failure of the MPPT system used to condition the only power source of the satellite definitely falls into this category. As such, it is crucial that the MPPT system is designed to be as reliable as possible.

Designing an electronic system for reliable operation within a space environment requires a different approach than designing one for terrestrial use. First, there is no atmosphere in space, meaning that it is not possible to cool the components by means of natural convection. This can lead to over-heating if the system is not carefully designed.

The other troublesome phenomenon in space is ionizing radiation. Most electronic components are vulnerable when exposed to any radiation at all, and will inevitably fail if the exposure continues for long enough. The amount of radiation an electronic component is exposed to, termed the Total Ionizing Dose (TID), varies greatly depending on the application but can be successfully mitigated using shielding and the careful selections of components and housing techniques.

Single Event Effects (SEE), on the other hand, occur as a result of heavily-charged particles and cannot be mitigated by the use of shielding. They can cause digital circuits which rely on state machines to abruptly change states. This can cause devastating results within a complex element like a microcontroller. Not only that, SEE can also cause an electronic component to latch-up, which may permanently damage it.

In order to avoid the issues of operating within a space environment, we decided to design a whole system using only carefully selected analog components. The usual method of dealing with latch-ups caused by SEE is to cut the power to the system when they occur, thus preventing permanent damage. This is not possible in this case, since the MPPT system is powered directly by the power source of the satellite. As such, all the components were selected based on their resistances to SEE.

In order to maximize the amount of power generated by the limited amount of solar panels on a satellite, the system needs to be as efficient as possible. Additionally, the less power that is dissipated in ways that are non-productive for the operation of a satellite, the less of an issue thermal management becomes.

B. Design constraints

We have designed our MPPT system so that it can be used for connecting one solar panel to one managed battery pack. The output of the system is protected by a diode, which allows multiple MPPT system instances to connect to a single battery pack without them interfering with one another. This increases the redundancy of the satellite because a failure of a single MPPT system instance does not prevent the satellite from generating power altogether but only decreases the amount generated. This further allows the satellites' designers to increase the performances of each MPPT system's instances

by optimizing their parameters for the solar panel connected to them.

The specific implementation described in this paper is optimized for a satellite in LEO. The constraints for the design were differentiated by studying the following two scenarios, applicable to a satellite orbiting in LEO.

The first scenario deals with a satellite under normal operating conditions. It periodically orbits the Earth over a period which is approximately 100 minutes. During that time, it encounters two areas of operation. The first begins when it exits the Earth's shadow. During this time, its solar panels begin to heat up, reaching up to 55 °C. All the time during this phase its solar panels are pointed towards the Sun, thus generating the power which is used to fill the batteries. Afterwards, it reenters the Earth's shadow, where all the power generation stops. During this time, the temperatures of the solar panels drop down to -40 °C.

The second scenario is analogous to the first, except that due to an unexpected failure of the satellite's attitude control system, it begins tumbling with a period of a few seconds. The temperatures rise and fall the same as in the first scenario but the illuminations of the solar panels vary greatly over time, as the satellite never locks the panels in the direction of the Sun.

By looking at these two scenarios the need for a system that can operate over a wide temperature range and which can track the MPP of a solar panel under rapidly varying conditions (satellites can tumble at rates of up to a few Hz) can be seen. Specifically, using commercially obtainable space grade solar panels with 8 W nominal power per panel, it can be concluded that the input voltage which such a system would need to handle lies between 15 V and 22 V, with input current reaching up to 0.5 A. The maximum input power would then be expected to be 9 W. Additionally, a battery pack consisting of 3 lithium cells connected serially was chosen, which has a voltage range spanning from 7.5 V to 12 V, with a maximum charge current to the battery pack of up to 1.2 A.

C. Analog MPPT implementations

As solar power is one of the more popular methods of generating renewable energy, there is a strong interest in researching new ways of making conversions from it more efficient. As a consequence, several of papers dealing with MPPT methods have recently been published (as of writing this paper, Google Scholar references more than 32,000 articles containing the keyword "MPPT"). This means that there are many different approaches to implementing MPPT algorithms, as well as many different MPPT algorithms themselves. Summarizing all the methods available within the published literature would warrant a separate paper altogether (e.g. [1]). Instead, this paper is focused only on those papers dealing with the analog implementations of MPPT algorithms.

Even when regarding only analog implementations there were a couple of approaches that had been proposed. One simple method included the use the OC voltage of a solar panel as an estimate of the MPP voltage. This could be implemented in different ways. One method would be to include an additional solar panel, which would be used to measure the OC voltage, thereby monitoring the current operating conditions of all solar panels [5]. The cost of including an additional solar panel to a satellite can be quite high, especially when using custom made solar panels, which is why this method was not particularly suitable for our needs.

It would also be possible to repeatedly disconnect the solar panel from the load when measuring the OC voltage [6]. This method was also not very suitable, as it required a complicated logical circuit for its operation. It would also be questionable as how it would perform under rapidly changing conditions.

Another implementation of an analog MPPT relies on the Ripple Correlation Control (RCC) method [7] [8]. This method measures the solar panel's current and voltage and then calculates the power generated using an analog multiplier. The power signal, and either the voltage or the current signal, are then differentiated using a differentiator circuit. The differentiated signals are first converted to discrete logic signals, which are then compared using an XOR gate. This output would then be used for the regulation of the solar panel's operating point. While this method did have the reaction speed required, it also required a special analog multiplier. This was also not an ideal solution, as analog multipliers are complex components which are quite cumbersome and there is little available data that would support their suitability for space applications.

Additionally, there are methods which function similarly to the RCC method but instead of deriving two signals only the solar panel power signal is differentiated. The control of the solar panel operating point is then performed on the basis of the current state of the MPPT algorithm and the derivative of the current power. Such a system, in addition to the analog multiplier, would also needs some kind of memory to store the current state, either by using a counter [9], or by means of a custom logic circuit [10] [11]. A similar method to this, which

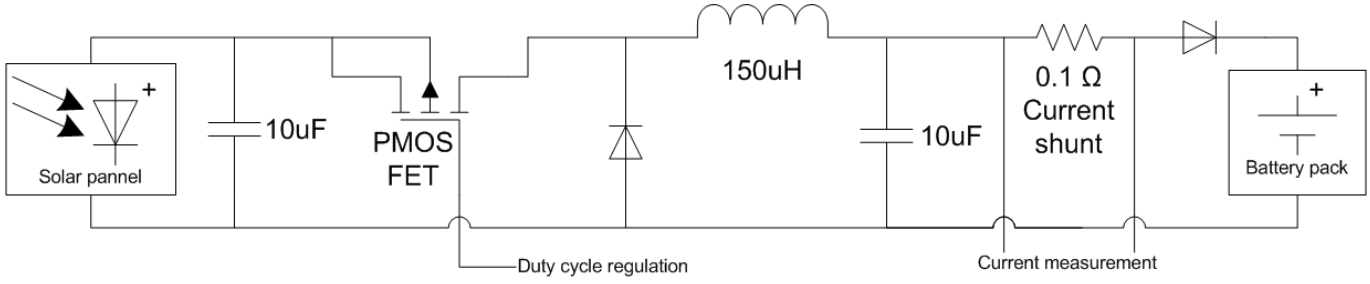

Fig. 3. Electrical schematic of the step-down switching power converter.

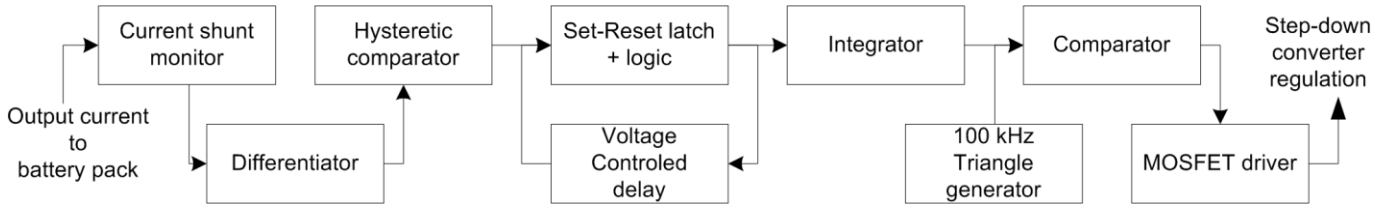

Fig. 4. Block diagram of the MPPT signal processing chain

requires a complex calculation, but instead measures only voltage parameters, is presented in [12].

There are of course analog MPPT methods which would perform remarkably well under the previously mentioned constraints. One example of such a method can be found in [13]. We have opted to avoid this method, as it requires the use of a complex power converter topology, such as a SEPIC or Ćuk converter. Since reliability is crucial for systems for use within a space environment, we feel that a simpler power converter topology is more appropriate for the proposed system. Another such method is described in [14], which requires two identical solar panels to function. The problem with this method is that it would require all solar panels to be connected together, which would detrimentally affect the operation of the system in the case of a single solar panel failure.

The final design of the proposed system is based on the method described above as shown in [11], though with significant changes to make it more suitable for use on LEO spacecraft. Primarily the described implementation was analyzed and modified to make it more suitable for operation within a space environment. Several components were exchanged as well as integrated within the system in the context of a spacecraft electrical power system. In this aspect, the proposed MPPT system is optimized to be used on a spacecraft with multiple smaller (approximately 10 W) solar panels, connected together to a single energy storage component – in a similar manner as shown in [15] except for situations where lower power is required.

Regarding the modifications to the MPPT algorithm, the analog multiplier was replaced by only measuring the output current, then using it to estimate the input power, as explained in [16] and [17]. The logic needed to perform this regulation was quite simple, thus enabling us to implement it in the form of a reliable analog circuit. The design was additionally extended with the addition of a variable delay by modifying the digital algorithm presented in [18] into an analog one and adjusting the delay time with regards to our MPPT system. The regulation loop was thereby prevented to become stuck in an extreme position, which occurred in certain circumstances (i.e. when the SC parameter of the solar panel is low). This was achieved by increasing the delay when it was too small to compensate the noise and transient effects present in the system while operating near an extreme position – when the duty cycle regulation can not be increased or decreased further. In addition, the variable delay increases the efficiency of the MPPT system by decreasing the response time of the regulation loop when operating at higher powers.

III. System Implementation

In accordance with the design constraints a simple switching converter was chosen to be used for the power conversion part of the MPPT implementation. The input voltages from the solar panels are always above the output voltages of the battery pack, which means that a step-down topology can be used. The MPPT algorithm is then implemented as an analog signal processing chain, which uses the output current signal to control the duty cycle of the step-down converter [19].

To summarize the design constraints as they differ from terrestrial MPPT implementations:

- The MPPT needed to be tracked in rapidly varying illumination and temperature conditions.
- Different component use was minimized to use only radiation tolerant components.
- The whole system needed to be implemented in an analog form with as little complexity as possible.
- The system must perform satisfactory even with small solar panels (down to 8W nominal power).

A. Step down switching power converter

There are a variety of possible switching power converters that could be used with the proposed system (e. g. [20] or even [21]), though we have opted to use a classic buck converter topology, as can be seen in Fig. 3. In contrast to the typical configuration, a P-type MOSFET transistor was used instead of the usual N-type. The filter values themselves were experimentally determined by minimizing the switching noise while keeping the system agile enough. This was done by initially using values from the system proposed in [11], then tuning them manually using the prototype.

TABLE I
VOLTAGE LEVELS PRESENT IN THE DESIGN

Voltage level	Function	Value
PGND	The ground of the whole satellite, negative terminals of the battery and the solar panel.	0 V
VCC	Voltage of the positive terminal of the solar cell.	PGND + 12 V to 22 V
GND	Ground of the signal processing chain, generated using a negative linear regulator.	VCC – 5 V
VREF	Virtual ground of the signal processing chain, generated using a resistive divider between VCC and GND.	VCC - 2.5 V
VOUT	Voltage of the positive terminal of the battery.	PGND + 7.5V to 11V.

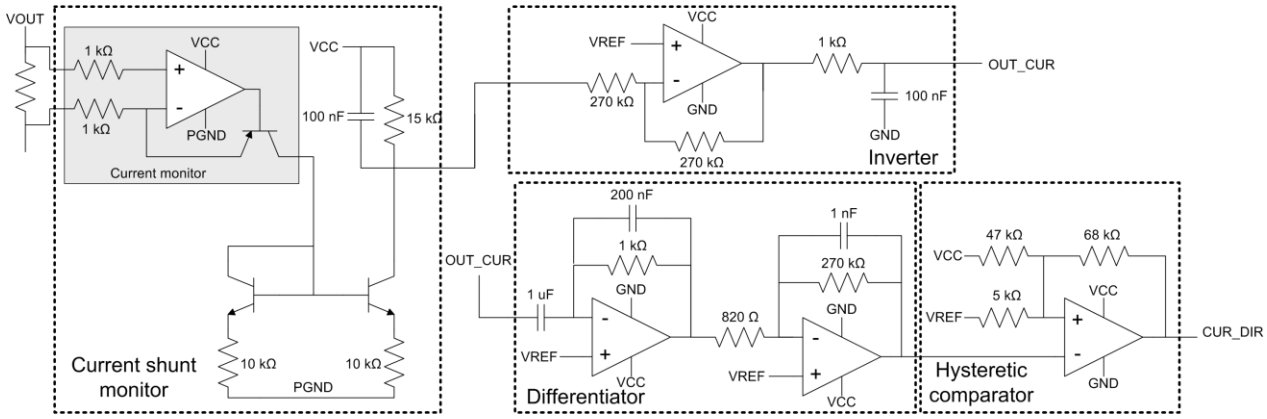

Fig. 5. Electrical schematic of the output current processing circuit.

B. MPPT signal processing chain

The signal processing chain itself is implemented as a collection of analog sub-circuits, as can be seen in Fig. 4. The main principle of operation is as follows. First, the output current of the power converter is measured, by which the current power generated by the solar panel is measured. This is a result of the fact that the output of the converter is fed to a battery, meaning that the output voltage is approximately constant (it changes very slowly, not fast enough to influence the operation of our algorithm). As such, by measuring the output current, the output power is directly measured, which is approximately equal to the input power. This current signal is then differentiated and its derivative compared with the virtual zero, allowing the system to decide whether the output current is increasing or decreasing. Based on this information a simple decision logic circuit with a delay is used in order to drive an error amplifier circuit. The output from the integrator circuit is then finally used to generate a Pulse-Width Modulated (PWM) signal which controls the power converter.

The signal processing chain uses 5 distinct voltage levels which are listed in TABLE I.

1) Output current processing circuit

The output current is measured by using a current shunt resistor, which is then converted to voltage using a high-side current monitor and a current mirror (see Fig. 5). This is necessary in order to allow us to shift the voltage levels between VOUT and VCC. The gain of the current monitor is set to provide the current signal with a voltage range of between GND and VREF, thus allowing us to use it for controlling the voltage-controlled delay circuit. The signal is then processed using a differentiating circuit and Operational Amplifiers (OP).

Finally, the differentiated signal is compared using a hysteretic comparator. This gives us a discreet signal, which is later used in the logic circuit. The comparator itself has a small hysteresis which is offset in the negative direction. This assures that the negative output level of the comparator is preferred, which is needed, so that the MPPT algorithm does not get stuck in an extreme position.

2) Decision logic circuit

The output from the hysteretic comparator is then input into the decision logic circuit, which consists of a Set-Reset (SR) latch and a voltage-controlled delay. The input signal is a logic signal with its voltage at VCC if the output current is increasing and at GND otherwise. What the decision circuit then does is to reverse the regulation direction whenever the input signal is at GND (meaning that the current is decreasing and the operating point is heading in the wrong direction on the solar panel's I-V curve). The circuit also features a delay, forcing the transient effects of a reversal to settle before a new reversal of regulation direction occurs.

The logic circuit itself consists of a SR latch constructed with an OP and passive components while other logic components are made from transistor logic, as can be seen in Fig. 6. Such an unconventional design was chosen to avoid using logic ICs due to radiation concerns. The logical function implemented with the logic circuit can be seen in Fig. 8.

During the initial testing of the MPPT system, it was noticed that the stability of the whole system was influenced

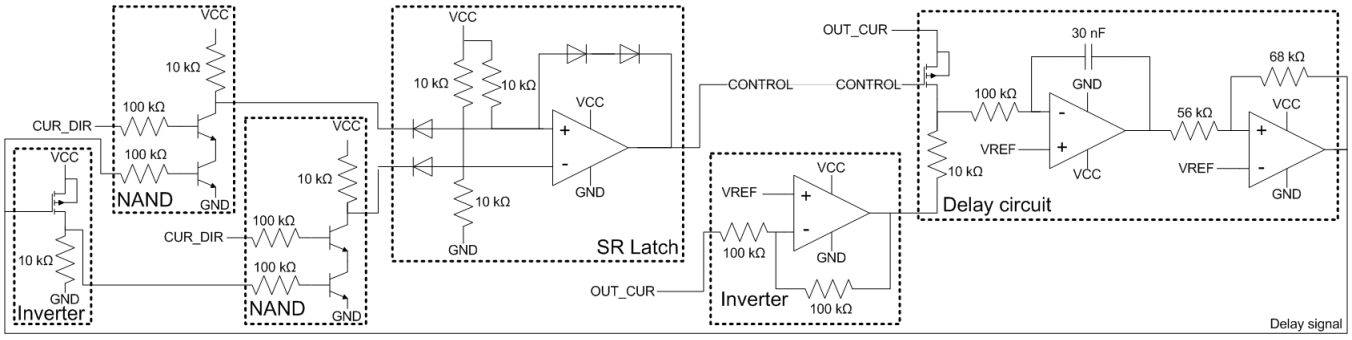

Fig. 6. Electrical schematic of the decision logic circuit

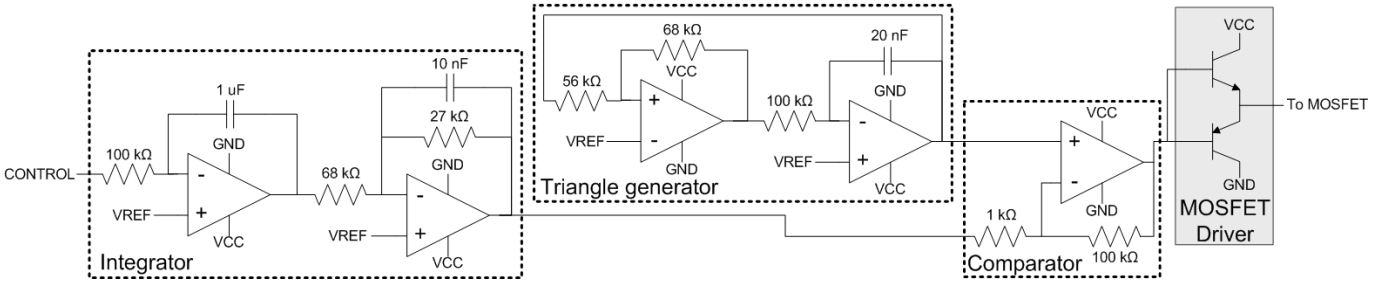

Fig. 7. Electrical schematic of the power converter regulation circuit

by the delay. As such, the delay was implemented so that it scales in relation to the output current, which was described in the previous chapter.

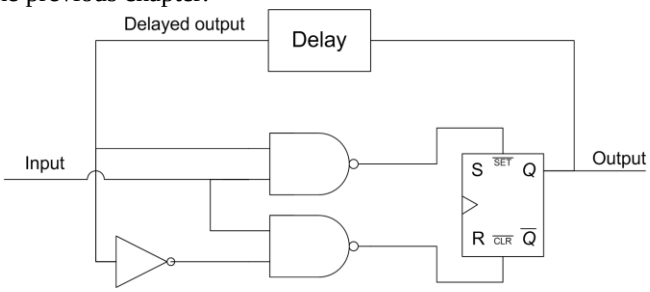

Fig. 8. Logic function implemented by the decision logic circuit.

The delay was implemented using 3 OPs, two of which configured as a modified oscillator without the feedback, while the third OP inverts the output from the current monitor (see Fig. 6 for details). The output from the current monitor and its inverted signal are then used to drive the oscillator circuit, the higher the voltage of the signal, the faster the switch occurs. This means that the delay induced by the decision logic circuit is longer when the output current is small, while the delay decreases when the output current gets bigger.

The optimal delay time was determined by trial and error during the testing of the system prototype. The value of the RC constant (The capacitor and resistor of the delay circuit in Fig. 6) was increased until the system ceased to lock itself in an extreme position when connecting and disconnecting the battery pack. In case the input or output specifications of the solar panel or battery would change, the RC value would need to be adjusted so, that the delay at low output currents remains large enough to allow the system to begin tracking the MPP even in the case that it drifts to an extreme position. Since other parameters of the MPPT would also need to be modified, the specifics of this modification are beyond the scope of this paper.

3) Power converter regulation circuit

The final part of the MPPT system is tasked with generating the PWM signal which drives the step-down switching converter in accordance with the output from the logic circuit (see Fig. 7). The output of the logic circuit is used to increase or decrease the duty cycle. In order to perform this function, two OPs are used, one as an integrator and the other as an inverting amplifier. The output from the integrator is then directly proportional to the duty cycle of the PWM signal with which we drive the MOSFET of the power converter.

In order to generate the PWM signal a classic oscillator with two OPs is used. The first generates a 100 kHz triangle signal, which is then compared with the integrator output signal, using the other OP. The 100 kHz switching frequency was selected primarily based on component availability (lower frequencies would require large capacitors and inductors). This frequency also limits the amount of high frequency noise generated and is also low enough so that the PWM generator can be constructed using only OPs.

The PWM signal is then finally used to control the power converter, using a MOSFET driver. The reason why a negative regulator was used to generate the voltage range for the signal processing chain is that it allows the driver to drive the P-type MOSFET using this simple configuration, without exceeding the maximum Gate-Source voltage of the MOSFET.

C. Part selection

As has already been stated in this paper, careful component selection was needed to ensure that the proposed system can perform as expected within a space environment. In accordance with this, a list of all the components needed to construct this system was compiled. The focus was on the latch-up tolerances of the components, as these are the most critical points of failure throughout the whole system. TID ratings were also checked, but due to the fact that the system is targeted at LEO, most components can presumably be tolerant to the TID present there. This applies especially to all passive components, diodes and bipolar transistors which can be presumed immune to a TID of up to 30 krad [22]. This means that the life-times of these components in LEO cover at least 3 years.

TABLE II
PARTS USED

Part	Function	Latch-up tolerance
OPA2835	Low power operational amplifier used for most of the signal processing chain.	TI SOI BiCOM process, latch-up immune.
LM137	Negative linear regulator.	Passed tests for radiation effects.
MIC4416	MOSFET driver	Latch-up tolerant by design.
AD8212	High side current monitor	Commercial version of radiation hardened part.

This table lists all parts that were specifically selected for our system. For parts not listed a generic version was used, as the part is innately immune to latch-ups.

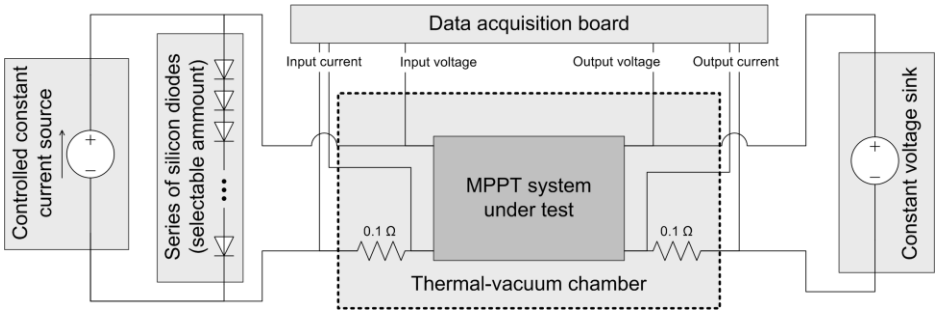

Fig. 9. Measurement setup for the MPPT system performance characterization. The series of silicon diodes is used to vary the OC voltage parameter, while the controlled constant current source is used to vary the SC current parameter. Currents are measured by applying 0.1 ohm shunt resistors near the ground, to avoid over-voltage issues with the data acquisition board.

With respect to latch-up tolerance, we limited the design to only use P-type MOSFET transistors and NPN-type bipolar transistors, as these types are more latch-up tolerant than their complements [23]., This is a consequence of P-type MOSFETs being produced on a P-type substrate, thereby avoiding a possible thyristor configuration which can become active in the presence of radiation, as is the cause with N-type MOSFETs.

Additional commercially-available components were identified, specifically OPs, which are fabricated using a complimentary Silicon on Insulator (SOI) process, being inherently latch-up immune [24]. No similar comparator components were identified, which is why only OPs are used in the design.

In regard to specific components, the negative linear regulator selected has been radiation tested [25]. The MOSFET driver was also radiation tested, specifically against latch-up effects [26]. The high-side current monitor was selected to be a commercial version of a radiation hardened part [27].

IV. Experimental results

In order to evaluate the performance of the MPPT system, a measurement setup was devised which consists of: a power source emulating the characteristic of a solar panel, a data acquisition board to measure the input and output powers of the MPPT system, a constant voltage active load which acts as a battery pack and a thermal-vacuum chamber, inside which the system was subjected to conditions that emulate a space environment. The whole measurement setup can be seen in Fig. 9.

The power source was constructed using a controlled constant current source in parallel with a series of silicon diodes. The characteristics of this setup are very close to those of various solar panels, allowing control of the SC current parameter (via the controlled current source) and the OC voltage parameter (via the number of diodes connected in series) of the power source.

A NI USB-6343 DAQ was used as the data acquisition instrument. The input and output currents of the MPPT system were measured using 0.1 ohm shunt resistors, while the voltages were measured differentially. All the measurements were performed inside a thermal-vacuum chamber, at a pressure of roughly 0.1 mPa. The measurements were performed at three distinct temperatures: at -25 °C, at 30 °C and at 85 °C. The voltage at the output was fixed at 10 V using the constant voltage active load.

A. Static performance

The first batch of measurements was performed in order to evaluate the static performance of the MPPT system. The OC

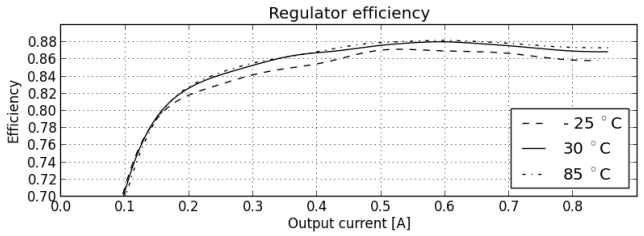

Fig. 10. Averaged measured static regulator efficiency

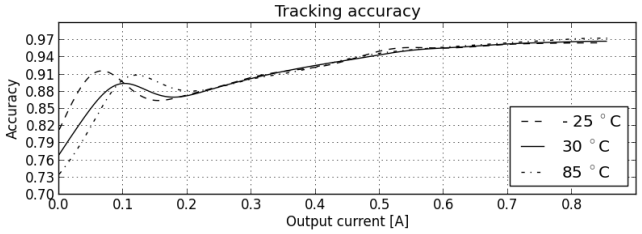

Fig. 11. Averaged measured static tracking accuracy

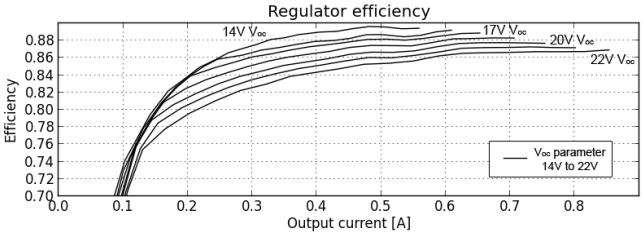

Fig. 12. Measured static regulator efficiency at 30°C

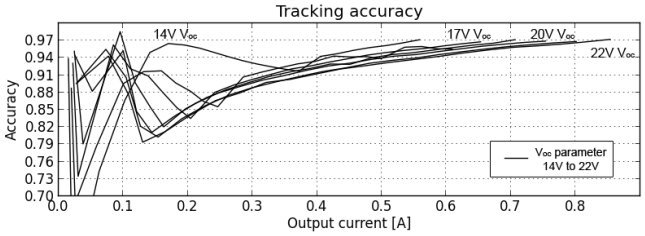

Fig. 13. Measured static tracking accuracy at 30°C

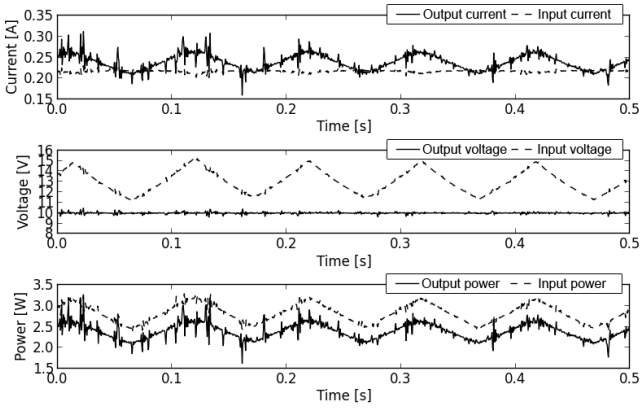

Fig. 14. MPPT system static measurements (dashed lines are input parameters) – 30 °C, 240 mA SC current, 18.5 V OC voltage

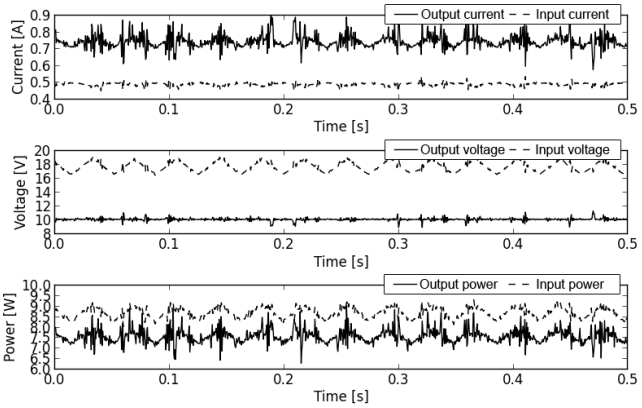

Fig. 15. MPPT system static measurements (dashed lines are input parameters) – 30 °C, 500 mA SC current, 22.5 V OC voltage

voltage and SC parameters were varied so that the system was exposed to input currents of up to 500 mA and to an input voltage range of 14 V to 22 V. The system remained functional during the whole measurement process.

In order to characterize the system, two parameters were calculated from the measured data. First we calculated the regulator efficiency, which is a measure of how much power is lost to heat within the MPPT system. The tracking accuracy of the MPPT system, which is a measure of how much power is actually drawn from the solar panel with regard to the maximum amount of power available, was also calculated.

As can be seen in Fig. 10 and Fig. 11, the regulator efficiency of the system at its operating point (7 W output) varied at around 88 %, while the tracking accuracy varied at around 96 %. It can be seen that the regulator efficiency slightly increased with temperature. It was also highly dependent on the input voltage, which is shown in Fig. 12. The efficiency also increased with increased output power. These losses occurred mainly within the signal processing chain part of the system, which requires more than 20 mA of current to remain operational. This was the reason the efficiency dropped at higher input voltages, as a higher voltage meant more power was dissipated on the linear regulator. It was also the reason for the increase in efficiency while increasing the output power.

The other parts of the losses occurred on the transistor and the diodes of the switching regulator. This was the reason the efficiency increased with increasing temperature, as the power dissipation of such components decreased with temperature.

The tracking accuracy, on the other hand, remained almost unchanged with increasing temperature and was less dependent on the input voltage (see Fig. 11 and Fig. 13). The tracking accuracy increased rapidly with increasing output currents – this was the effect the voltage-controlled delay has on the MPPT system.

Fig. 14 and Fig. 15 illustrate the workings of the MPPT system. It can be observed that the output current was greater than the input current, while the input voltage was higher than the output voltage. The triangular-shaped perturbations of most parameters, which were a result of the MPPT being tracked, are shown. It can be clearly seen that the perturbation period decreased with increased output power.

It should be noted that the oscillations of the input voltage and output current are an inherent part of the operation of the proposed MPPT system. Though it would be possible for the MPPT system to vary the delay time with regards to the magnitude of the change of output current (as proposed in [28]), we feel that this would increase the complexity of the proposed MPPT system too much – the use of the voltage-controlled delay already limits the loss of the tracking accuracy when operating at high output power, where the loss of tracking accuracy due to the oscillations would be most detrimental. This can be seen in Fig. 11, where the loss of tracking accuracy is less than 3% when operating at the highest rated output current.

B. Dynamic performance

In accordance with the scenarios applicable to a small satellite in a LEO (as defined in previous chapters) a dynamic test of the MPPT system was performed. This was done by, firstly, varying the SC current parameter in the shape of a half-rectified sine wave and later in the shape of a full-wave rectified sine wave, which closely mirrored the conditions encountered by either a single-sided or double-sided solar

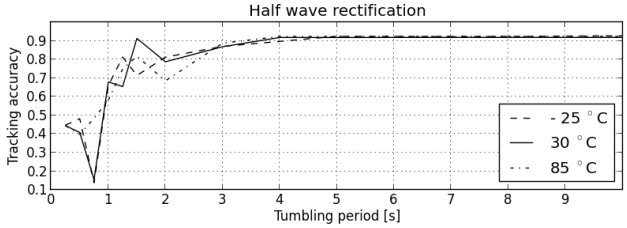

Fig. 16. Measured dynamic half-rectified sine wave tracking accuracy

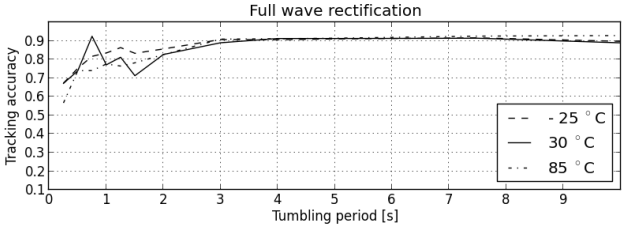

Fig. 17. Measured dynamic full-rectified sine wave tracking accuracy

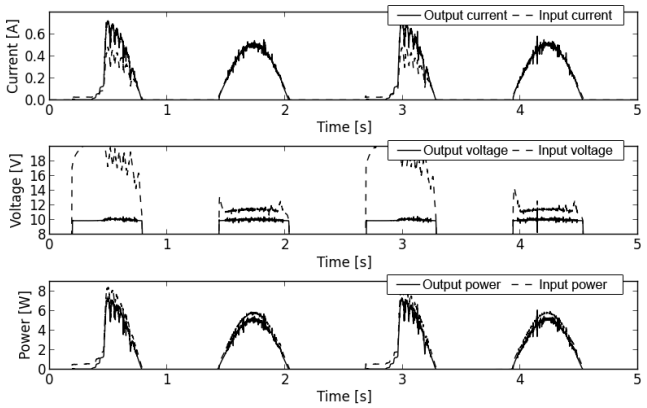

Fig. 18. MPPT system dynamic measurements– half wave rectification, 30 °C, 1.25 s period

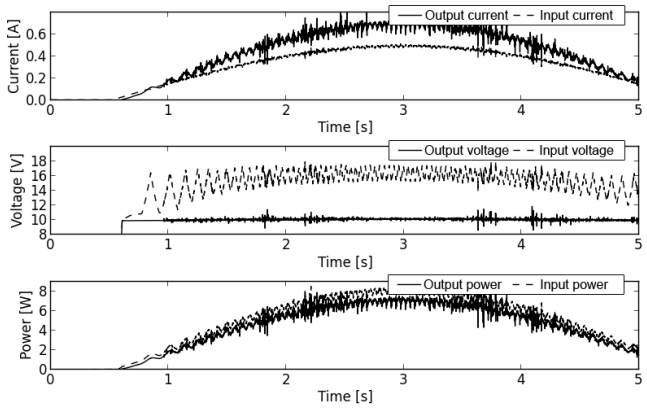

Fig. 19. MPPT system dynamic measurements – half wave rectification, 30 °C, 10 s period

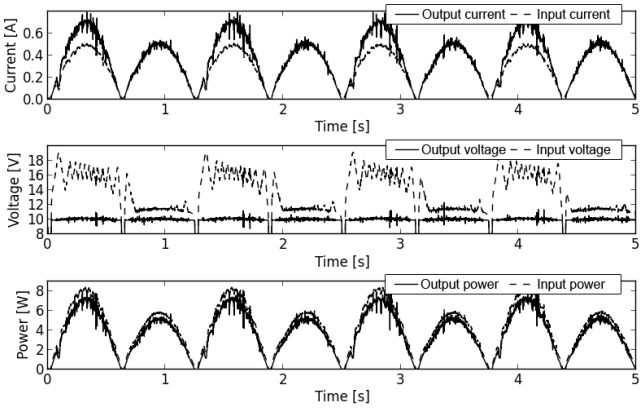

Fig. 20. MPPT system dynamic measurements – full wave rectification, 30 °C, 1.25 s period

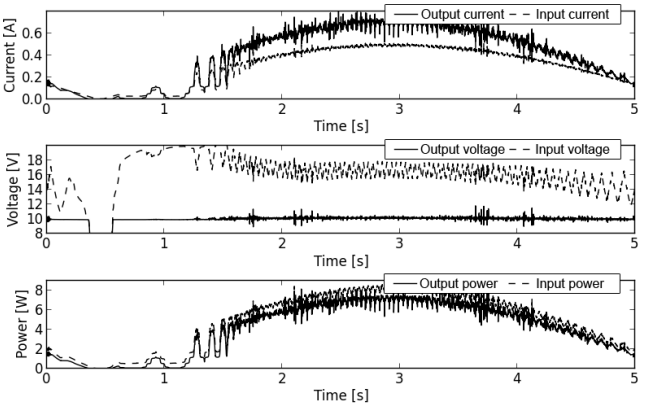

Fig. 21. MPPT system dynamic measurements – full wave rectification, 30 °C, 10 s period

panel tumbling around its axis. The periods of the sine wave were varied from 0.25 second to 10 seconds and the tracking accuracy of the system was measured.

As can be seen in Fig. 16 and Fig. 17, the system tracked the MPP of a solar panel even under dynamic conditions. When the conditions changed with to a frequency of less than 0.5 Hz, the system was capable of tracking the MPP almost perfectly, with deviations near those areas of steep changes within the operating conditions of a solar panel. The tracking accuracy during such conditions is above 90 %.

It can also be seen that there was in fact a difference in the performance of the system when tracking a half-rectified sine wave (which is a simulation of a solar panel facing only one side of the satellite) and when tracking a full-rectified sine wave (which is a simulation of two solar panels on a satellite, facing opposite directions). At frequencies higher than 0.5 Hz, the system was much better at tracking a fully-rectified sine wave than a half-rectified sine wave. The reason for this was the fact that during half-wave rectification, when no current was being supplied to the system it ceased to function due to the lack of power. When the output current started to increase it began to function again, but it took a short time interval before the MPP was accurately tracked again. This effect can be seen in Fig. 18.

At higher frequencies the tracking accuracy decreased since the system periodically tracked the MPP incorrectly, as can be seen in Fig. 18 and Fig. 20.

Another interesting effect occurred at low frequencies (an example being the 0.1 Hz frequency sine wave), where the fully-rectified sine wave input had a lower tracking accuracy. This is a consequence of the system becoming underpowered for a short time when the input sine wave dropped below the supply voltage of the system. After the sine wave increased again, a short time interval passed before the MPP was successfully tracked again (see Fig. 19 and Fig. 21). This did not happen with the half-rectified sine wave, as the system had time to completely power off in-between the periods.

The two effects described above could be mitigated by keeping the system constantly powered from the battery pack by omitting the output diode. This feature would come at the expense of no isolation between the MPPT systems, decreasing the reliability of the power system. Furthermore, the power consumption of the power system would inadvertently rise, as the MPPT units would be powered even when no power is produced by them. Additionally, if the isolation between MPPT systems is not needed, a better approach might be to connect all solar panels to a single MPPT system, as described in [29].

V. Conclusion

This paper proposed a design for a reliable analog maximum power point tracking system for use on a satellite within LEO. The design takes into account most of the environmental effects which a system is typically exposed to,

as well as the parameters of a typical 7 W solar panel.

The proposed system was then prototyped and had its performance evaluated using a specially built measurement setup, also described in this paper. The results suggested that the system performed as expected, tracking the maximum power point of the solar panels successfully during testing.

There were two possible improvements to the system that we identified. Firstly, the system had 88 % regulator efficiency at its operating point. This could be increased further by designing a system which uses more efficient operational amplifiers and comparators, which we had failed to identify. Another improvement would be with regard to the tracking accuracy, which was roughly 96 % at the operating point. We presume that it could be further increased by replacing the 100 kΩ resistor of the delay circuit with a non-linear resistor, thus decreasing the delay further at higher output currents. Further improvements could be achieved by compensating the noise present in the system, as proposed in [30].

However, the current implementation of the MPPT system combines good power conversion performance with high system reliability. Though some of the performance was sacrificed in order to achieve a high level of reliability, this sacrifice is justified, as the single most important characteristic of any system to be used within a space environment, is its reliability. However, the system's performance remained comparable with the currently available functionalities of similar products, while offering improved radiation tolerance, decreased complexity, and excellent tracking accuracy.

REFERENCES

[1] T. Esram and P. L. Chapman, "Comparison of photovoltaic array maximum power point tracking techniques," *Energy Convers. IEEE Trans. On*, vol. 22, no. 2, pp. 439–449, 2007.

[2] P. C. Adell, A. F. Witulski, R. D. Schrimpf, F. Baronti, W. T. Holman, and K. F. Galloway, "Digital control for radiation-hardened switching converters in space," *Aerosp. Electron. Syst. IEEE Trans. On*, vol. 46, no. 2, pp. 761–770, 2010.

[3] N. Fermia, D. Granozio, G. Petrone, and M. Vitelli, "Predictive & adaptive MPPT perturb and observe method," *Aerosp. Electron. Syst. IEEE Trans. On*, vol. 43, no. 3, pp. 934–950, 2007.

[4] T. Senjyu, K. Uezato, and others, "Feedforward maximum power point tracking of PV systems using fuzzy controller," *Aerosp. Electron. Syst. IEEE Trans. On*, vol. 38, no. 3, pp. 969–981, 2002.

[5] A. Tariq and J. Asghar, "Development of an analog maximum power point tracker for photovoltaic panel," in *Power Electronics and Drives Systems, 2005. PEDS 2005. International Conference on*, 2005, vol. 1, pp. 251–255.

[6] J. Ahmad and H.-J. Kim, "A voltage based maximum power point tracker for low power and low cost photovoltaic applications," *World Acad. Sci. Eng. Technol.*, vol. 60, pp. 712–715, 2009.

[7] M. Savenkov and R. Gobey, "A simple maximum power point tracker utilizing the ripple correlation control technique," in *ISES-AP–3rd International Solar Energy Society Conference–Asia Pacific Region, Incorporating the 46th ANZSES Conference*, 2008.

[8] S. L. Brunton, C. W. Rowley, S. R. Kulkarni, and C. Clarkson, "Maximum power point tracking for photovoltaic optimization using ripple-based extremum seeking control," *Power Electron. IEEE Trans. On*, vol. 25, no. 10, pp. 2531–2540, 2010.

[9] C.-Y. Yang, C.-Y. Hsieh, F.-K. Feng, and K.-H. Chen, "Highly efficient analog maximum power point tracking (AMPPT) in a photovoltaic system," *Circuits Syst. Regul. Pap. IEEE Trans. On*, vol. 59, no. 7, pp. 1546–1556, 2012.

[10] Z. Liang, R. Guo, and A. Huang, "A new cost-effective analog maximum power point tracker for PV systems," in *Energy Conversion Congress and Exposition (ECCE), 2010 IEEE*, 2010, pp. 624–631.

[11] R. Leyva, C. Alonso, I. Queinnec, A. Cid-Pastor, D. Lagrange, and L. Martinez-Salamero, "MPPT of photovoltaic systems using extremum-seeking control," *Aerosp. Electron. Syst. IEEE Trans. On*, vol. 42, no. 1, pp. 249–258, 2006.

[12] M. Veerachary, T. Senjyu, and K. Uezato, "Voltage-based maximum power point tracking control of PV system," *Aerosp. Electron. Syst. IEEE Trans. On*, vol. 38, no. 1, pp. 262–270, 2002.

[13] K. K. Tse, M. T. Ho, H. S. Chung, and S. R. Hui, "A novel maximum power point tracker for PV panels using switching frequency modulation," *Power Electron. IEEE Trans. On*, vol. 17, no. 6, pp. 980–989, 2002.

[14] J.-H. Park, J.-Y. Ahn, B.-H. Cho, and G.-J. Yu, "Dual-module-based maximum power point tracking control of photovoltaic systems," *Ind. Electron. IEEE Trans. On*, vol. 53, no. 4, pp. 1036–1047, 2006.

[15] J. M. Blanes, A. Garrigos, J. A. Carrasco, A. H. Weinberg, E. Maset, E. Sanchis-Kilders, J. B. Ejea, and A. Ferreres, "Two-stage MPPT power regulator for satellite electrical propulsion system," *Aerosp. Electron. Syst. IEEE Trans. On*, vol. 47, no. 3, pp. 1617–1630, 2011.

[16] M. Momayyezan and H. Iman-Eini, "Maximum power point tracking for photovoltaic arrays with minimum sensors," in *Power and Energy (PECon), 2010 IEEE International Conference on*, 2010, pp. 911–916.

[17] D. Shmilovitz, "On the control of photovoltaic maximum power point tracker via output parameters," in *Electric Power Applications, IEE Proceedings-*, 2005, vol. 152, pp. 239–248.

[18] C. Cabal, C. Alonso, A. Cid-Pastor, B. Estibals, L. Seguier, R. Leyva, G. Schweitz, and J. Alzieu, "Adaptive digital MPPT control for photovoltaic applications," in *Industrial Electronics, 2007. ISIE 2007. IEEE International Symposium on*, 2007, pp. 2414–2419.

[19] D. Selčan, G. Kirbiš, and I. Kramberger, "Analog implementation of an output current based solar cell maximum power point tracking algorithm for use on the TRISAT mission," in *Electrotechnical and Computer Science Conference ERK 2013. Twenty-Second International*, Portorož, Slovenija, 2013, vol. 22, pp. 203–204.

[20] T.-F. Wu, C.-H. Chang, and Y.-J. Wu, "Single-stage converters for PV lighting systems with MPPT and energy backup," *Aerosp. Electron. Syst. IEEE Trans. On*, vol. 35, no. 4, pp. 1306–1317, 1999.

[21] O. Garcia, P. Alou, J. A. Oliver, D. Diaz, D. Meneses, J. A. Cobos, A. Soto, E. Lapena, and J. Rancano, "Comparison of Boost-Based MPPT Topologies for Space Applications," *Aerosp. Electron. Syst. IEEE Trans. On*, vol. 49, no. 2, pp. 1091–1107, 2013.

[22] D. Sinclair and J. Dyer, "Radiation Effects and COTS Parts in SmallSats," in *Proceedings of the 27th AIAA/USU Conference on Small Satellites*, 2013.

[23] M. Maher, *Radiation Owners Manual - Issues, Environments, Effects*. National Semiconductor Corporation, 1999.

[24] Unknown, "TI Space Products Components for Extreme Environments," *Texas Instruments*, 2013. [Online]. Available: http://www.ti.com/lit/pdf/sgzt006.

[25] K. Sahu, "TOTAL DOSE CHARACTERIZATION TESTS PPM-97-043," *NASA*, 1997. [Online]. Available: http://radhome.gsfc.nasa.gov/radhome/papers/tid/PPM-97-043.pdf.

[26] M. D. Skipper, K. Atkins, G. R. Hopkinson, and K. A. LaBel, "Radiation effects in Micrel MIC4427 MOSFET drivers," in *Radiation Effects Data Workshop, 1995, NSREC'95 Workshop Record., 1995 IEEE*, 1995, pp. 50–54.

[27] Unknown, "Single Event Latchup Testing of the AD8212 High Voltage Current Shunt Monitor for Analog Devices," *Radiation Assured Devices*, 2010. [Online]. Available: http://www.analog.com/static/imported-files/generic_radiation_reports/AD8212S_SEL_generic.pdf.

[28] E. M. Ahmed and M. Shoyama, "Novel stability analysis of variable step size incremental resistance INR MPPT for PV systems," in *IECON 2011-37th Annual Conference on IEEE Industrial Electronics Society*, 2011, pp. 3894–3899.

[29] M. Miyatake, F. Toriumi, N. Fujii, H. Ko, and others, "Maximum power point tracking of multiple photovoltaic arrays: a PSO approach," *Aerosp. Electron. Syst. IEEE Trans. On*, vol. 47, no. 1, pp. 367–380, 2011.

[30] H. Al-Atrash, I. Batarseh, and K. Rustom, "Effect of measurement noise and bias on hill-climbing MPPT algorithms," *Aerosp. Electron. Syst. IEEE Trans. On*, vol. 46, no. 2, pp. 745–760, 2010.

David Selčan was born in 1990 and received his B.Sc. and M.Sc. degree in electronic engineering from the University of Maribor, Slovenia in 2012 and 2014 respectively. He is currently working towards his Ph.D. degree in electronics engineering.

His research and work experience include participation in various projects since 2010, which includes the European Student Moon Orbiter project.

His research interests include digital and embedded system design, signal processing, space technologies, and biomedical electronics.

Gregor Kirbiš was born in 1990 and received his B.Sc. and M.Sc. degree in electronic engineering from the University of Maribor, Slovenia in 2012 and 2014 respectively. He is currently working towards his Ph.D. degree in electronics engineering.

His work experience has included participation in various projects since 2010, which includes the European Student Moon Orbiter project.

His research interests include RF engineering, space technologies, signal processing and brain-computer interfaces.

Iztok Kramberger (M'99-VM'09) was born in 1973 and received his B.Sc., M.Sc., and Ph.D. degrees from the University of Maribor, Slovenia, in 1997, 2001, and 2003, respectively, all in electrical engineering.

He has been a valued IEEE member for 16 years. He currently works as an assistant professor and since 2009 has headed the Laboratory for Electronics and Information Systems at the Faculty of Electrical Engineering and Computer Science.

His research work extends into the fields of computer vision, brain-computer interfaces and space technologies. He has experience in embedded system design, programmable logic devices and electronic systems.